

## 21.3 A 65nm CMOS 1-to-10GHz Tunable Continuous-Time Lowpass Filter for High-Data-Rate Communications

Fawzi Houfaf<sup>1,2</sup>, Mathieu Egot<sup>1</sup>, Andreas Kaiser<sup>2</sup>, Andreia Cathelin<sup>1</sup>, Bram Nauta<sup>3</sup>

<sup>1</sup>STMicroelectronics, Crolles, France, <sup>2</sup>IEMN / ISEN, Lille, France, <sup>3</sup>University of Twente, Enschede, The Netherlands

As of today, the highest cut-off frequency low-pass continuous time analog filters are in the frequency band of 1 to 3 GHz [2,4-6], targeting applications like UWB communications or hard disk drives. Nevertheless, bands much higher, of about 10GHz, are to be addressed in the near future. This paper demonstrates an active low-pass filter tunable from 1 to 10GHz in 65nm CMOS, which is to our knowledge the highest ever cutoff frequency reported.

In this work the Gm-C topology was adopted for its merits at high frequencies. In this technique, two critical parameters should be accounted for: the accuracy of the Q-factors of the poles pairs (for correct transfer function) and parasitic capacitances (for maximal cut-off frequency). The former point is influenced by the phase shift of the integrators compounding the filter in the neighborhood of the filter's edge frequency. This phase error is due to two antagonistic effects which are the integrator's finite DC gain and its high frequency poles/zeros. The gm-C integrator in Figure 21.3.1 [1] performs a minimized phase shift thanks to the absence of internal nodes hence getting rid of high frequency poles responsible for phase lead with respect to the ideal  $-90^\circ$ , and a negative resistance technique boosting the DC gain which is responsible for phase lag. Due to the absence of internal nodes, the integrator's unity gain frequency and DC gain can be tuned with  $V_f$  and  $V_q$  respectively. In the early 90's, this method allowed achieving cutoff frequencies of 100MHz in  $3\mu\text{m}$  CMOS, while here we investigate its limits in 65nm CMOS.

The gyrator synthesis method, starting from a doubly terminated LC-ladder prototype, was used for its simplicity, modularity and for gate-drain capacitances cancellation which otherwise would generate zeros responsible for additional integrator phase shift. The node B in figure 21.3.1 showed a voltage swing 1.8 times higher than the other nodes, thus the 4 transconductors gm4, gm5, gm6 and gm7 were doubled and the capacitor multiplied by 4. This allows halving the voltage peak at the internal node, keeping the Cgd cancellation effect, and being able to absorb a parasitic capacitance 4 times higher at this node compared with a non-scaled version. To compensate the 6dB inherent loss of a doubly terminated prototype and also by foreseeing some insertion loss due to process back-end the input transistor was multiplied by 3 instead of the conventional factor 2.

At the transistor level and in order to minimize parasitic capacitances, the 4 inverters implementing common-mode feedback and negative resistance (inverters b, c) were dimensioned at the minimum size that still guarantees common-mode (CM) stability. CM stability for this filter topology requires to size the inverters such that  $(g_{mb}+g_{mc}) \geq 0.66 g_{ma}$ . This theoretical limit (0.66) was verified by simulation; however during design a margin of 10% was taken. It should be noticed that traditionally in the transistor  $g_{ma} \sim g_{mb} \sim g_{mc}$ , this means that our optimization allowed more than 120% parasitic capacitance saving at each node which roughly doubles the highest achievable operation frequency and saves power. Also shorted negative feedback transconductors simulating the resistors in the passive prototype were replaced by bare inverters in the same concern of reducing parasitic capacitance and power dissipation.

For the third order LPF as a rule of thumb the integrator DC gain (or gm/go of a transistor) needs to be  $\sim 100$  and the effective parasitic pole has to be a factor  $\sim 100$  above the filter cutoff frequency. We aim here for 10GHz cutoff frequency so the effective parasitic pole of the transistor should be in the range of 1THz. This requires extensive modeling and design of all parasitic effects, including non-quasistatic transistor modeling. At the complete layout level extensive use of electromagnetic simulator was adopted, as each parasitic R,L,C effect has an important impact on the filter transfer function.

Minimizing the interconnects resistance and complying with electro migration (EM) industrial reliability rules imposed the use of wide tracks and stacking of metallization layers. An optimized inverter structure is shown in Figure 21.3.2 where a 3pmos2nmos structure turned out to be the optimum from inductance minimization point of view. The PMOS and NMOS transistors were interleaved to enhance even more EM reliability. Also ground shielding techniques borrowed from electromagnetic compatibility engineering and a ground network

has been adopted to allow electrons to pick their return path, naturally choosing the one which cancels out connection inductance at high frequencies.

All these layout techniques have the drawback of increasing the capacitive effects. We could however achieve a cutoff frequency of 10GHz at typical supply voltage condition using for all integration capacitances only the parasitic ones. Filter operation above 8GHz necessitates a tuning voltage  $V_f > 1.2\text{V}$ . It has nevertheless been carefully checked that no thin oxide device in the design was overpassing the reliability voltage breakdown limits on any junction.

For measurement sake an inverter-based buffer was appended at the output of the filter, and an impedance matching network was plugged at the input and output. A reference path, including the same buffers and matching network was as well integrated on chip, in order to de-embed the filter transfer function. The chip photomicrograph is given in Figure 21.3.7; it occupies an active area of  $0.01\text{mm}^2$  in a LP 65nm CMOS.

Measurements show S-parameters which correspond exactly to the ideal passive LC prototype (see figure 21.3.3). The Q-tuning was performed manually, it shows 1dB gain, 1.2 dB ripple, a notch was observed at around 8 times the cutoff frequency probably due to a coupling between signal lines via dummy fillers which had not been completely extracted. Varying  $V_f$  shows a large tuning range from 0.6 to 10GHz.

The filter measured performances are provided in figure 21.3.6 for several cut-off frequency operation modes, and compared with relevant state of the art. The IIP3 measurements are reported for edge of the band signal tones (25MHz spacing), while the noise measurements are performed over the filter pass-band using a wide-band instrumentation amplifier at the output. All the presented figures are de-embedded with respect to the input and output access elements thanks to additional measurements on the reference path.

The obtained measured performance in terms of noise and linearity, even at the record cut-off frequency of 10GHz, well outstands the existing state of the art. The generic power per pole per Hz figure of merit permits to compare the different implementations. For the same energy efficiency as the work presented in [3], the presented work exhibits  $\sim 5$  times larger cut-off frequency for the same noise behavior and an edge of band IIP3 15dBc better. From an applicative perspective, in the case of 10GHz high data rate optical links, an SNR of 36dB is requested which the presented work out-performs with a margin of 9dB.

This paper has demonstrated the feasibility and robustness of up to 10GHz LP CT filters in deep submicron CMOS processes, with excellent noise and linearity behavior and with a continuous cut-off frequency tuning capability of over a decade.

### Acknowledgments:

Special thanks go to C. Arnaud and P. Scheer from ST, D. Ducatteau and team from IEMN and G. Wienk from UTwente.

### References:

- [1] B. Nauta, "A CMOS Transconductance-C Filter Technique for Very High Frequencies", *IEEE Journal of Solid-State Circuits*, Volume: 27, Issue: 2, 1992
- [2] Terada, T.; Yamawaki, T.; Kokubo, M.; Nasu, K.; "100–1000 MHz cutoff frequency, 0–12 dB boost programmable Gm-C filter with digital calibration for HDD read channel", *Proceedings of ESSCIRC*, 2009, Page(s): 108 - 111
- [3] P. Wambacq, V. Giannini, K. Scheir, W. Van Thillo, Y. Rolain, "A fifth-order 880MHz/1.76GHz active lowpass filter for 60GHz communications in 40nm digital CMOS", *Proceedings of the ESSCIRC*, 2010, Page(s): 350 – 353
- [4] Baranauskas, D.; Zelenin, D.; Bussmann, M.; Elahmadi, S.; Edwards, J.; Gill, C.; Tran, K.; Linder, L.; Tan, H., "A 6th Order 1.6 to 3.2GHz Tunable Low-Pass Linear Phase gm-C filter for Fiber Optic Adaptive EDC Receivers", *Radio Frequency Integrated Circuits Symposium*, 2009, Page(s): 495 – 498
- [5] V. Saari, M. Kallio, S. Lindfors, J. Ryyanen, K.A.I Halonen, "A 240-MHz Low-Pass Filter With Variable Gain in 65-nm CMOS for a UWB Radio Receiver", *IEEE Transactions on Circuits and Systems I: Regular Papers*, Vol. 56, Issue 7, pp.1488 – 1499, July 2009
- [6] Harrison J., Weste N., "A 500 MHz CMOS anti-alias filter using feed-forward op-amps with local common-mode feedback," *2003 IEEE International Solid-State Circuits Conference*, Digest of Technical Papers, pp. 132-483 vol.1, 2003

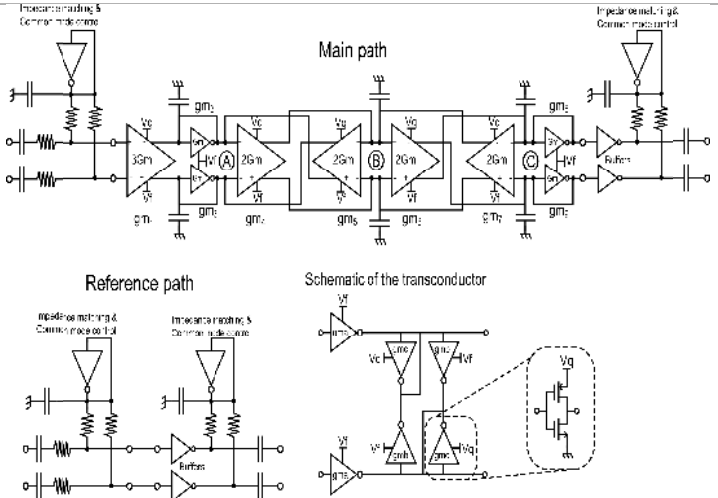


Figure 21.3.1: Gm-C filter implementation (main path, top), reference path (bottom left) and transconductor schematic (bottom right)

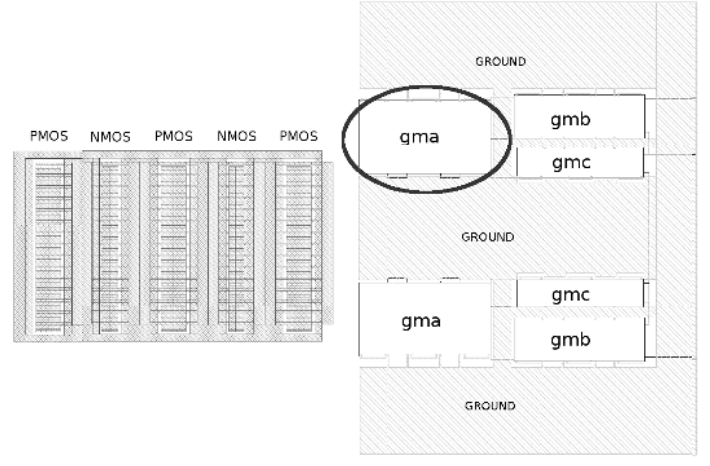


Figure 21.3.2: Partial layout floor plan of a single inverter (left) and transconductor (right)

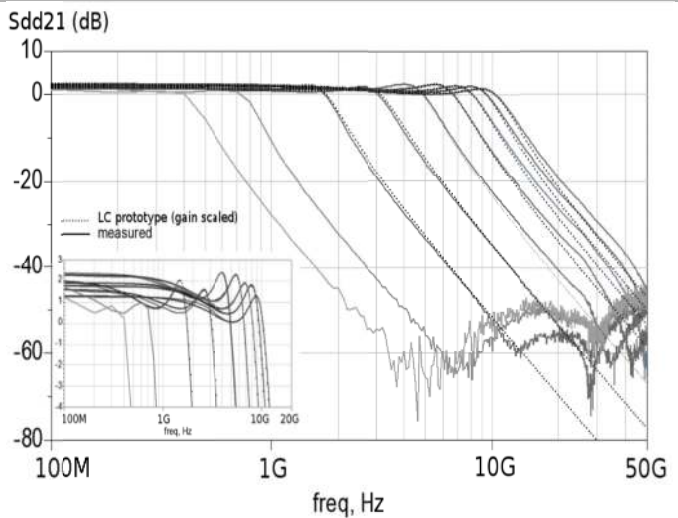


Figure 21.3.3: Measured differential S parameters (solid) and comparison with the ideal LC prototype filter (dashed)

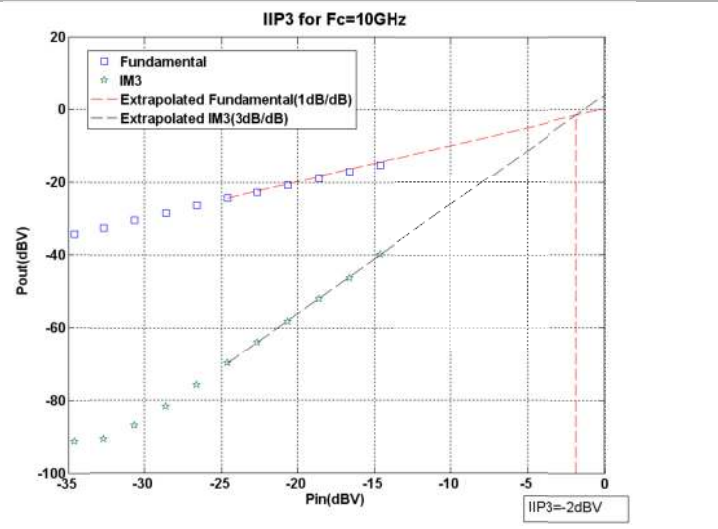


Figure 21.3.4: Measured filter IIP3 for  $F_c = 10\text{GHz}$  (edge of the band tones with spacing 25MHz)

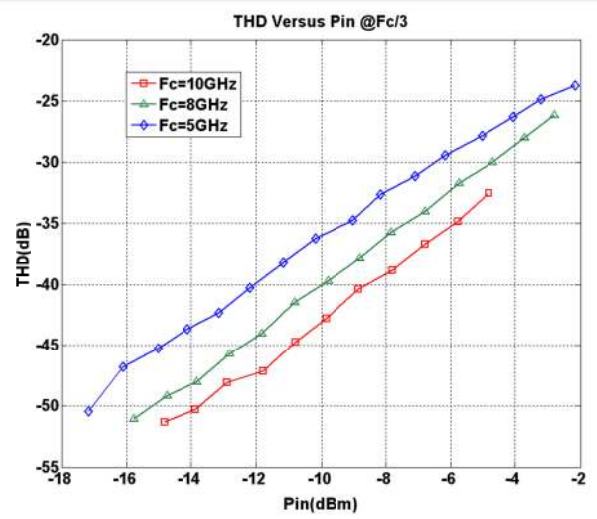


Figure 21.3.5: Measured Total Harmonic Distortion at  $F_c/3$  for  $F_c = 5, 8$  and  $10\text{GHz}$

Parameter	This work $F_c=4.7\text{GHz}$	This work $F_c=7.9\text{GHz}$	This work $F_c=10\text{GHz}$	[3]	[4]	[5]	[6]
Process	65nm CMOS	65nm CMOS	65nm CMOS	40nm CMOS	0.18 $\mu\text{m}$ SiGe	65nm CMOS	0.18 $\mu\text{m}$ CMOS
Vdd (V)	1	1.2	1.4	1.1	3.3	1.2	1.8
Topology	Gm-C	Gm-C	Gm-C	Sallen-Key biquad	Gm-C	Gm-C	Active-RC
Type	Chebyshev	Chebyshev	Chebyshev	Butterworth		Chebyshev	Elliptic
Order	3	3	3	5	6	5	5
$F_c$ -3dB (MHz)	4700	7900	10000	1760	3000	275	500
In-band gain (dB)	2.7	2	1.3	0	---	9 ... 43	0
Input PSD (nVrms/√Hz)	6.61	5.92	5.02	6	---	7.8	18
In-band IIP3 (dBVp)	-3	-2.5	-2	-18	-2.85	-12.5	13.5
THD @ xx Vpp diff input	-45dB@ 160mVpp	-45dB@ 200mVpp	-45dB@ 264mVpp		-40dB @ 0.9Vpp		-40dB @ 1.73Vpp
SNR (dB)		42	45				
Total Power (mW)	19	60	140	21	300	36	90
Power per pole per Hz (mW/GHz)	1.34	2.53	4.66	2.38	16.66	26.18	36
Active area (nm <sup>2</sup> )	0.01	0.01	0.01	0.0392	0.17	0.21	---

Figure 21.3.6: Measured Filter performances for several cut-off frequencies and comparison with state of the art